Thermal lensing in ocular media exposed to continuous-wave near-infrared radiation: the 1150–1350-nm region

Rebecca L. Vincelette
Ashley J. Welch
University of Texas
Department of Biomedical Engineering
1 University Station, C0800
Austin, Texas, 78712

Robert J. Thomas
Benjamin A. Rockwell
Air Force Research Laboratory
Human Effectiveness Directorate-Optical
2624 Louis Bauer Dr.
Brooks City-Base, Texas, 78235

David J. Lund
U.S. Army Medical Research Detachment
7965 Dave Erwin Dr.
Brooks City-Base, Texas 78235

Abstract. Ocular damage threshold data remain sparse in the continuous wave (CW), near-infrared (NIR) radiation region save for the 1300-nm area that has been investigated in the past several decades. The 1300-nm ocular damage data have yielded unusual characteristics where CW retinal damage was observed in rabbit models, but never in nonhuman primate models. This paper reviews the existing 1300-nm ocular damage threshold data in terms of the fundamental criteria of an action spectrum to assist in explaining laser-tissue effects from near-infrared radiation in the eye. Reviewing the action spectrum criteria and existing NIR retinal lesion data lend evidence toward the significant presence of thermal lensing in ocular media affecting damage, a relatively unexplored mechanism of laser-tissue interaction. © 2008 Society of Photo-Optical Instrumentation Engineers. [DOI: 10.1117/1.2978066]

1 Introduction

The near-infrared (NIR) region defined here as the range from 1150 to 1350 nm is unique in terms of potential hazards to the cornea and retina. Near-infrared wavelengths in this region have penetration depths on the order of $700 \ \mu$m; long enough to easily pass through the cornea, but short enough that <5% of the total intraocular energy reaches the retina.[1–3] At these wavelengths, there is little change in the linear absorption coefficient with temperature.[4] Nevertheless, there should be sufficient energy reaching the retina to ensure retinal lesions for a collimated beam entering the eye without damage to the cornea. Experimental safety studies in the 1300-nm regime find retinal damage thresholds for single-pulse exposures of 50 ns to 650 μs in rhesus subjects, while continuous wave (CW) exposures of 0.1 to 10 s can produce corneal lesions, but never retinal damage.[5–11] However, analogous experiments performed on rabbits cause retinal damage. This anomaly of CW retinal damage lesions between species has only been observed in this particular wavelength region. The key wavelength-dependent factors affecting retinal threshold damage are (*i*) the percent of laser light reaching the retina, (*ii*) the spot size of the laser beam at the retina, and (*iii*) the relative absorption by the pigment epithelium (PE) in the retina.

We hypothesize that significant thermal lensing of the 1300-nm beam protects the retina. In this paper, the optics and retinal threshold data for rabbits and nonhuman primate animal models, as well as exposure limits, are reviewed. Experimental and modeling results are presented to support the hypothesis of enlarged retinal spot size owing to thermal lensing in the eye at 1300 nm and the implications this has for exposure limits to NIR wavelengths.

Existing exposure limits spanning a wide range of wavelengths over several decades can be found in the literature. Much of these data are reflected in standards by the American National Standards Institute in the Z136 series, which provides guidelines on safe levels of exposure for various tissues and wavelengths and by the International Commission of Non-Ionizing Radiation Protection.[12,13] Parameters such as beam size at the cornea, beam divergence, pupil diameter, exposure duration, pulse repetition rate, and multiple wavelength exposures all influence damage threshold data. Unfortunately, these parameters are not well characterized for regions in the NIR where water absorption becomes significant.[3] Accurate damage predictions in this region require rigorous investigational studies of ocular damage thresholds where a multitude of parameters are considered. Threshold ocular damage is typically thermal in nature with the most important wavelengths being those that reach the retina.

2 Background

Retinal damage threshold studies have been conducted for wavelengths ranging from the ultraviolet (UV) to the infrared (IR) for CW down to the ultrashort femtosecond pulses.[5–7,10,13–16]. Numerous studies have branched from the retinal damage cases to observe discrete laser-tissue mecha-

Address all correspondence to Rebecca L. Vincelette, University of Texas, Department of Biomedical Engineering, 1 University Station, C0800, Austin, Texas 78712. Tel. 512-799-2332; Fax. 210-536-3903; E-mail: rebecca.vincelette@gmail.com
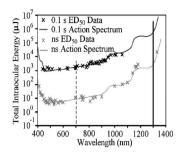
Fig. 1 The action spectrum for the rhesus eye for ns and 0.1-s exposures compared to corresponding experimental retinal ED_{50} data thresholds.[7,68] Reprinted with permission from Zuclich et al.[7]

nisms influencing the process, such as beam shape, retinal spot size, and exposure duration.[16–24]

Typically, the primate is preferred for more meticulous retinal damage studies due to its eyes' close similarities to human eyes while a lesser species, the rabbit, is suitable for corneal damage studies and some retinal damage studies.[5,6,8,10,16,19,25–30] Experiments using primates to evaluate retinal damage thresholds use a sedated subject; after the eye is cyclopleged and dilated, it is exposed to an incident laser beam of a selected wavelength for a predetermined length of time.[5,6,10,25] For retinal studies at any wavelength, the laser beam is typically passed through an aperture set to a diameter of ~5 mm for NIR and 3 mm for visible wavelengths, just before the cornea. The input beam diameters are kept small enough to avoid clipping of the pupil and aberration effects while still allowing the beam to focus in the animal model's natural position with a nonaccommodated eye. As a result, chromatic aberrations are not corrected; longer wavelengths are focused at a more posterior retinal location than shorter wavelengths. The beam's power is recorded as the amount of power entering the eye and represented as the total intraocular energy (TIE). Retinal damage is assessed by using a fundus camera to observe the presence or absence of a lesion in a carefully marked and recorded grid on specific areas of the retina. If the lesion is visible, then the size of the lesion can be estimated ophthalmoscopically or measured through histopathology. Probit analysis is used to determine the estimated damage (ED) threshold where damage occurs 50% of the time, known as the ED_{50}, for a specific wavelength and TIE.[31] The lesion data are then related to exposure duration, corneal beam profile, elapsed time postexposure, and other parameters. Once the ED_{50} is determined, the maximum permissible exposure is set with a safety margin from three to 1000, depending on wavelength, exposure duration, and predicted retinal spot size from trends in experimental measurements. The damage observed at the retina can be divided into three classes: injury resulting from photochemical, thermal, or thermomechanical processes.[20,32]

Zulich et al.,[7] Lund et al.,[17] and Lund and Edsall[21] have developed a process for expressing a theoretical fit to the TIE ED_{50} data as a function of wavelength based upon thermal and thermochemical ocular-tissue properties. Though not by conventional definition, they refer to this theoretical fit as an action spectra. Their action spectra for the retinal hazard wavelengths (400–1400 nm) for 50-ns and 0.1-s exposures are compared to experimental data in Fig. 1.[7,17,21]

The inherent complexities involved in the creation of their action spectra are best described by Lund and Edsall as a "simplistic model of the laser/tissue interactions and that the fit may be, in part, fortuitous."[21] It should be understood that the action spectra is a heuristic approximation to ED_{50} data. Nonetheless, the algorithm for creating the action spectra described by Lund et al. provides a classic foundation for an elemental analysis of laser tissue interaction in ocular media.[33]

The calculation for the Lund et al.[17,21,33] action spectra is first referenced to a fixed data point using the experimentally determined ED_{50} minimum visible lesion (MVL) for 700-nm laser radiation at 50-ns and 0.1-s exposure durations, marked by the dashed vertical line in Fig. 1. Below 1200 nm, the 50-ns exposures fall within the thermal impulse response of the retinal pigment epithelium (RPE) to laser irradiation and the 0.1-s exposures approach the steady-state thermal response.[34] The ED_{50} estimates for all wavelengths, other than 700 nm, are then calculated based on three fundamental criteria: (*i*) absorbance of the RPE and water, (*ii*) transmission of the light to the retina, and (*iii*) the predicted spot size at the retinal plane primarily based on chromatic dispersion models. The greatest uncertainty with damage predictions of NIR radiation is the spot size of the laser beam at the retina and the role of the PE absorption in heating the retina.

The action spectra for 0.1-s and nanosecond exposure durations have been shown to fit the respective TIE data well for wavelengths below 1200 nm.[7] A gap in data exists between 1064 and 1350 nm, leaving this area of the NIR largely unexplored. The solid vertical line in Fig. 1 marks the only area in this gap, the 1300-nm region, which has been investigated. Studies investigating retinal damage between 1300 and 1340 nm have revealed puzzling data that do not fit existing methods for computing the action spectra for CW exposures.[6,8,35]

MVL studies for the retina at wavelengths between 1300 and 1340 nm, conducted by researchers at Brooks Air Force Base, Texas found minimum visible lesions on the retina for pulse durations of 650 μs or less in rhesus studies.[6,7,10] Retinal lesions were not observed for exposures of >650 μs on the same species. In the rhesus, damage was observed in other portions of the eye for CW cases before any damage was created at the retina.[8] Though retinal damage from a 1300-nm CW exposure with >650 μs duration was never achieved in studies using rhesus primates, the same laser conditions caused retinal damage in rabbits. For a summary of retinal and corneal damage threshold studies, see Tables 1 and 2, respectively.

In corneal damage studies, the laser beam is typically brought to a small spot, ~1 mm diam, converging at the cornea. Zuclich et al.[9] report corneal damage at 1318 nm involved the full corneal thickness unlike earlier studies by Zuclich et al.[36] in the far IR, where corneal damage only involved the epithelium layer. In studies for 1315–1356 nm involving CW (0.1–1 s) exposures, damage was observed at multiple sites throughout the eye, including the cornea, lens, iris, and retina in the rabbit.[9] Similar observations were made in the rhesus save for the fact damage was never observed at the retina. Zuclich et al.[9] also found the formation of cataracts in both rhesus and rabbit subjects when the incident power at

Table 1 ED_{50} (reported for retina as a TIE) values for retina from 1315 to 1330 nm. The TIE is the reported ED_{50} value from literature. The TIE was calculated based on TIE times the approximate area at cornea. The percent transmission was calculated from data reported by Refs. 2, 6–8, and 10 and can be found in Table 3.

Species	Wavelength (nm)	Pulse Duration	Approx. Beam Diameter Entering Cornea[a] (mm)	TIE: ED_{50} (J)[b]	TIE (W/cm²)[c]	Predicted %T to Retina	Refs.
Rhesus	1319	50 ns	4.5	0.0193	2.43×10^{06}	3.02	6 and 7
	1315	350 μs	5	0.334	4.86×10^{3}	3.78	6–8
	1330	650 μs	5.5	0.356	2.31×10^{3}	1.39	6, 7, and 10
Rabbit	1318	0.28 s	5	~34	6.18×10^{2}	6.75	6 and 8
	1318	0.69 s	5	~34	2.51×10^{2}	6.75	7 and 8
	1318	10 s	5	>370	1.88×10^{2}	6.75	7 and 8

[a]Note this measurement is taken in reference to the aperture placed some distance in front of a subject's cornea. The actual beam size entering the eye is unknown.
[b]TIE—Actual energy at cornea entering eye (assuming no clipping)
[c]This is the energy assumed to enter the eye at the cornea calculated by the formula: (TIE/Pulse Duration)/($\pi \times$ beam radius at cornea²)

the cornea was 260 J/cm² for CW (~0.25 s) exposures. Formation of the cataract was frequently observed to occur as two lesions in the eye, separated by a region of normal tissue, the first being an axially shallow lesion located at the anterior surface at the capsule, wherein the tissue immediately posterior to this lesion appeared normal. The second lesion exhibited significant axial depth and involved up to one-third of the total lens thickness. The longer cortical cataracts were noted to have an axially tapered lesion diameter. Zuclich et al.[8]

reported no such cortical cataracts with very few subjects yielding anterior subcapsular cataracts for studies involving 350 μs pulses.[8] In these 350-μs studies, damage through the anterior tissues of the eye was only observed when the beam was brought to a small spot of 1 mm or less at the surface of the cornea.

In NIR retinal ED_{50} studies, Zuclich et al.[36,38] described the 1318-nm lesion process as involving the full retinal thick-

Table 2 ED_{50} values for cornea from 1315 to 1356 nm.[6–11]

Species	Wavelength (nm)	Pulse Duration	ED_{50} (J/cm²)	Corneal Spot Size (mm)	ED_{50} (W/cm²)	Lens Threshold Relative to Cornea[b]	Sources
Rhesus	1318	0.28 s	72	1	2.57×10^{2}	1.8	6, 7, and 9
	1318/1338[a]	250 μs	45	0.4	1.80×10^{5}		10 and 11
	1318/1338[a]	5 s	212	1.4	4.24×10^{1}		7 and 11
	1356	0.33 s	81	0.7	2.67×10^{1}	5	7 and 9
Rabbit	1315	350 μs	42	1	1.20×10^{5}		6–8
	1318	0.69 s	175	1	2.54×10^{2}	0.75	7 and 9
	1318	10 s	1890	0.8	1.89×10^{2}		6–8
	1319	50 ns	540	0.15	1.08×10^{10}		6 and 7
	1356	0.22 s	58	0.7	2.64×10^{2}	2	7 and 9

[a]40% 1318, 60% 1338. MPE based on 1330 nm.
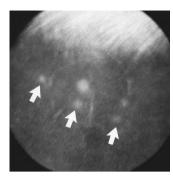[b]This value is a scalar; multiply by corneal ED_{50} for Joules/centimeters squared.

Fig. 2 Fundus image of a rabbit subject.[35] The arrows indicate the 514-nm marker lesions. Lesions adjacent to the marker lesions are from CW (exposure lengths of 1–10 s) 1318-nm NIR exposures as they appeared 24 h postexposure. Zuclich et al. speculated that the argon lesions measured 200 μm diam. This image first appeared in Zuclich et al.[35]

ness, which caused a late inflammatory response. A typical NIR retinal lesion did not appear within the first hour postexposure.[8,9,35,37] By 24-h postexposure, the NIR lesions were evident, characterized by a larger more reflective spot compared to the argon marker lesions. NIR, 1300-nm retinal lesions for 1–10 s exposures are shown in comparison to argon threshold lesions in Fig. 2.

The NIR lesions appeared to stabilize after 48 h.[35,37,38] By comparison, the argon marker lesions were always immediately visible after the exposure and did not change significantly in appearance over time. The argon wavelength has much higher absorption within the RPE compared to the 1318-nm wavelength lesions. Pathology and imaging of MVL lesions from this NIR region revealed minor damage reaching into the choroid with damage centering on the outer neural layer (ONL).[35,37] Swelling in the RPE was found to be much less in the 1318-nm NIR MVL studies compared to visible wavelength lesions. Zuclich et al.[35] reported subthreshold 1318-nm NIR MVL retinal exposures in rabbit subjects that were not viable in standard fundus camera observation, but were evident upon imaging with SLO at 780 nm. Histology of these subthreshold lesions, 48 h postexposure, revealed some swelling in the inner retina, slight vacuolization in the RPE, and dark nuclei in the ONL.

In observations made as long as two months postexposure, the NIR MVL shapes were irregular and large.[37] At three months postexposure, the larger area of inflammation was no longer observed and the smaller circular lesion observed at 24 h appeared again.

Clearly, laser-tissue interaction in the eye is a complicated process. The results from the 1300-nm studies leave many mechanisms of laser-tissue interaction in ocular media unexplained. One of these unexplained mechanisms is the role of thermal lensing in ocular media. Lin[23] and Lin et al.[24] explored the nonlinear thermal absorptive properties of the eye in the 1990s. The studies established the thermal lensing effect is dependent on wavelength, absorption, and exposure duration for several biological tissues.

Thermal lensing, also known as thermal blooming, is a well-known phenomenon discovered in 1965 by Gordon et al.[39] Thermal lensing is typically the result of a radial temperature gradient caused by the absorption of laser radiation along the beam path. In addition, axial absorption causes local changes in the index of refraction. As the temperature, T, in ocular media increases, density, ρ (mass/volume), decreases. This causes the index of refraction, n, along the beam path to become spatially dependent on the thermal distribution in the media. Thus, for a Gaussian beam profile, the temperature rise is largest at the center of the beam, meaning the index of refraction at a depth z is at a minimum on the beam axis and at a maximum along the outer edges of the thermal profile. The path the light takes through the ocular media causes the formation of a negative lens, which changes the spot size and subsequent focal position of the beam at the retina. Any change in the spot size at the retina directly impacts the local rate of heat generation. Understanding the role of thermal lensing in ocular damage mechanisms will allow for more accurate predictions of damage thresholds to establish a quantitative link between safety and efficacy for laser technologies.

3 Analysis

Perspective on the role of thermal lensing on damage thresholds in the NIR region from 1150 to 1350 nm can be gained by examining the three fundamental criteria used by Lund et al.[17,21,33] in developing the action spectra in Fig. 1.

3.1 Criteria 1: Absorbance of the RPE and Water Content of the Retina in the NIR Wavelength Region

Though some fluorophores and their isomers have been studied, to date, the absorptive properties of the RPE in the NIR are left largely unknown.[40–44] Numerous physiological changes occur in the aging RPE, including a reduction in cell density and changes in pigmentation.[45] One cause in the pigmentation change is from lipofuscin, a fatty by-product of metabolic processes containing pigments, which accumulates in RPE cells over time.[40] Lipofuscin buildup is just one example that can cause variability in optical absorption between species and subjects. In lieu of these facts, characterization of reported fluorophores, such as eumalanin, has revealed a significant decrease in absorption toward longer wavelengths.[41,42,44] Given the variability in pigmentation content and density of the retina between subjects, a trend in absorption of the RPE, neural retina and choroid in the NIR is a suitable analysis. In the 1960s to 1980s, Gabel et al.,[46] Coogan et al.,[47] Geeraets et al.,[48,49] and Birngruber et al.,[50] sought to measure the absorption of the PE over a variety of wavelengths; finding a large decrease in absorbance at longer wavelengths. To develop the action spectra in Fig. 1, Lund et al.[17,21,33] determined the data from Gabel-Birngruber et al.[46,50] yielded the best fit to MVL data. A least-squares fit to the Gabel-Birngruber et al.[46,50] data is found in the following (see Fig. 3):

$$458 \exp(-4.3 \times 10^{-3} \lambda), \qquad (1)$$

where the wavelength, λ, is in nanometers. A more detailed fit used in the action spectrum by Lund et al. uses the general form for PE absorbance as $1 - \exp(-\mu_a s)$ with all wavelengths normalized to the RPE absorption at 380 nm,[51] where s is the path length of the melanin granules, set to 5 μm, and
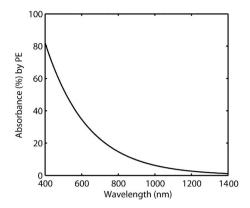
Fig. 3 A fit to the absorption data of rhesus PE from Birngruber et al. from Eq. (1).[50]

μ_a is the linear absorption coefficient calculated by $\mu_o(\lambda_o/\lambda)$.[3,5] The λ_o is the normalizing wavelength of 380 nm with a corresponding μ_o of 4100 cm^{-1}.

In the visible region, threshold lesions remained centered on the RPE, though suprathreshold exposures damaged the full-retinal thickness. In contrast, NIR threshold lesions involving full-retinal thickness and late-onset inflammation were not observed at visible or UV wavelengths.[35]

In general, the sensory retina is mostly transparent to retinal hazard wavelengths.[32] Though the RPE is approximately only 5 μm thick, it is rich with melanin granules and is believed to absorb nearly 50% or more of the energy in the visible range. In contrast, wavelengths in the NIR penetrate into the choroid, which contains blood vessels and some melanin granules. Geeraets et al. reported bulk absorbance of human retina and choroid over a broad spectrum finding a mean value of approximately 35–40% absorbance in the 1200–1400 nm region.[49] Considering the results from Geeraets et al.[49] and the fit to the Gabel-Birngruber et al.[46,50] data in Fig. 3, a trend can be seen where PE absorption decreases in the NIR while bulk absorption of the whole retina and choroid is much larger than in the RPE. It is reasonable to assume if
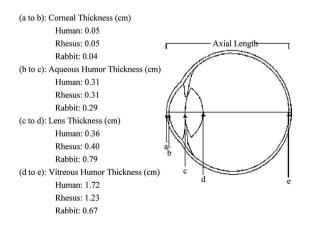

Fig. 4 Physiological data for eyes of three species represented as comparable schematic eyes.[52,53,69,70] Axial length is the sum of the distances from the front of the cornea at position a to the front of the retina at position e. Note the human lens thickness data include the cortex, core, and postcortex for a total lens.

Table 3 Percent of light transmission to RPE for rabbit, rhesus, and human eyes based on results from Fig. 6.

Wavelength (nm)	Rabbit	Rhesus	Human
1300	12.93	7.50	3.86
1315	7.74	3.83	1.65
1318	6.72	3.18	1.30
1330	3.35	1.27	0.40

denaturation occurs throughout the retina, owing to local heating of absorbed NIR radiation, then the average PE absorption coefficient is not significantly larger than the value of water in the NIR region. Denaturation of the retina from wavelengths in the NIR would not result from heat conducted from the RPE, which is the mechanism for retinal coagulation using laser radiation in the visible spectrum. Instead, denaturation of the retina is mainly due to the local water absorption of the NIR laser beam, with RPE absorption being only slightly higher.

3.2 Criteria 2: Transmission of Laser Radiation to the Retina

One of the differences between rabbit and rhesus in the 1300-nm retinal thresholds listed in Table 1 lies in the path length for each species. The axial length of an adult rabbit and rhesus eye are 17.9 and 19.9 mm, respectively.[52,53] Transmission losses include specular reflections and attenuation throughout the ocular media (refer to Fig. 4). Of course, the amount of 1300-nm laser radiation that reaches the retina is greater for the rabbit (see Table 3).

Absorption as a function of wavelength is slightly different for each portion of the eye as indicated by the measurements reported by Maher et al. (see Fig. 5) and follow closely to the absorption of water in the NIR region.[2,54] Absorption coefficients in the 1300-nm region for each ocular medium are reported in Table 4.

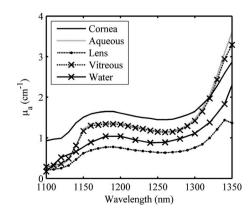For creating the action spectrum seen in Fig. 1, Lund and Edsall[21] reported using the values of Maher et al.[2] with

Fig. 5 Linear absorption coefficient, μ_a, as a function of wavelength for ocular media from rhesus eyes and water.[2,54]

Table 4 Linear absorption coefficient, μ_a (in centimeters), in the 1300–1330 nm region for ocular tissues interpolated from the data of Maher.[2]

	Wavelength (nm)			
	1300	1315	1318	1330
Cornea	1.65	1.92	1.98	2.28
Aqueous	1.47	1.90	2.01	2.54
Lens	0.761	0.92	0.97	1.21
Vitreous	1.42	1.80	1.90	2.43

approximately 5–10% transmission to the RPE layer at or near 1300-nm wavelengths.[21] If the physiological data from Fig. 4 are considered along with the linear absorption coefficients presented in Fig. 5, then Beer's law of attenuation can be applied to predict the percentage of light transmitted to the retina as seen in Fig. 6. Percent transmission values to the RPE for human, rhesus and rabbit in the 1300-nm region are reported in Table 3.

The fact that damage was induced at the retina in rhesus monkeys for 1330-nm exposures of 650 μs or less indicates there was sufficient transmission to the retina to cause damage in the rhesus, but does not explain why damage was not induced for CW exposures. Zuclich et al. reported the occurrence of anterior damage in multiple locations for both rhesus and rabbit in cases where the incident beam at the cornea was <1 mm.[8,9] Rabbit retina CW exposures were conducted at 1318 nm, and retinal lesions were observed.

To date, no other wavelength study has yielded such a discrepancy between species where CW retinal lesions could be seen in one but not the other. It is reasonable to assume physiological differences between species do contribute to the presence or absence of a lesion. However, these differences do not afford a complete explanation in the scope of all three
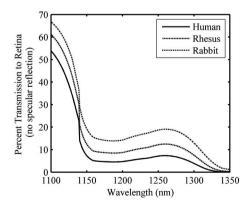

Fig. 6 Percent of transmitted light reaching the retina in the schematic eye from Fig. 4. Transmission values were calculated by Beer's law using ocular absorption values from Fig. 5 for respective ocular components. Calculations used here did not account for specular reflections at any boundary.

criteria to compute an action spectrum. Speculation on the impact of these physiologic differences on threshold data is saved for the discussion.

3.3 Criteria 3: Prediction of Spot Size Using Chromatic Dispersion Models

Lund et al. described the ratio of the diameter of the laser-beam spot formed at the retina with chromatic dispersion, d_λ, to that of the referenced MVL diameter, d_0, held as a constant as the only time-dependent quantity in the computation of the action spectrum shown in Fig. 1.[33] This ratio is expressed in the action spectrum computation by

$$\left(\frac{d_\lambda}{d_0}\right)^x, \tag{2}$$

where the power x ranges from a value of 2 for nanosecond pulses down to a value of 1 for 0.1 s or longer exposures. Typically, d_0 has been set to 25 μm, but some more recent studies suggest d_0 is two-to-three times larger.[25,55–57] Controversy has surrounded the value of x due to the discrepancy on the value of d_0.

In studies designed to determine the threshold for laser-induced retinal injury as a function of beam diameter at the retina, Lund et al. noted the appearance of a lesion diameter did not decrease for irradiance diameters less than 80–100 μm.[56] Some proposed hypotheses include forward-scattering properties of the eye, uncompensated ocular aberrations, and the fact that a RPE cell is ~13 μm diam. Essentially, the referenced MVL establishing the value for d_0 represents the diameter of the lesion formed on the retina after a threshold exposure to the reference wavelength of 700 nm. The lesion area found by fundus camera observation is seen as an area of changed appearance and believed to be created by the thermal profile induced in the tissue from the laser-beam's waist at the retina. Thus, if a minimum beam waist is predicted to be smaller than the value of d_0, theoretically, the MVL would still be no smaller than this referenced diameter. For this reason, Lund et al.[17] placed a lower bound of 40 μm on retinal spot size for their action spectra calculations.

To calculate d_λ, Lund et al.[17] and Lund and Edsall[21] use chromatic dispersion for a simple reduced eye model using the refractive error measurements from Wald and Griffen[58] and Bedford and Wyzecki.[59] More recent chromatic dispersion data, or refractive error, in the NIR for the human eye has been published by Fernandez et al.[60]

Chromatic dispersion of the human eye is typically represented by refractive error measurements, wherein all wavelengths are described by their relationship to a referenced wavelength of 589 nm.[61]

Refractive error, R [Diopters], is related to the reference focal length, f_o [m], and the focal length of other wavelengths, f [m], by

$$R = \left(\frac{1}{f_o}\right) - \left(\frac{1}{f}\right), \tag{3}$$

where $1/f_o$ is the power of the eye, D_o [Diopters], at the reference wavelength and $1/f$ is the power of the eye, D [Diopters], at the wavelength being compared.
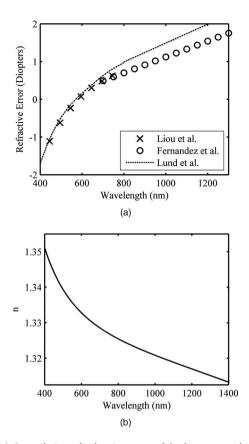
(a)

(b)

Fig. 7 (a) Compilation of refractive error of the human eye for several summary reports including an estimate of refractive error for computing the results by Refs. 17, 21, 60, 71, and 72. The linear fit from the Fernandez et al.[60] data was shifted to match the refractive error of the Liou et al.[71] model at 700 nm. (b) Result for $n(\lambda)$ based on the Liou et al.[71] and Fernandez et al.[60] data in (a). The Sellmeier fit to produce this result used the coefficients given in Table 5.

Thomas et al. use a reduced eye model with radius of curvature of 6.1 mm and $1/e^2$ Gaussian input beam diameter of 4.24 mm giving a focal length of 24.4 mm for the 589-nm wavelength.[62] Using this reduced eye model, a solution for the index of refraction as a function of wavelength can be found in a three step process. First, Eq. (3) is used to generate values for $f(\lambda)$ using the reduced eye model for f_o and the refractive error, R, values given by Liou et al.[71] and Fernandez et al.[60] The ABCD transform for a spherical-dielectric interface is then used with radius, $r=6.1$ mm, to converge upon a solution to $n(\lambda)$ with the index of refraction of air set to 1.0. Finally, a Sellmeier equation is fit to the result for $n(\lambda)$. The Sellmeier equation is then used to generate the ocular dispersion data needed for the reduced eye model. Figure 7(a) shows refractive error of the human eye, and Fig. 7(b) shows the resulting solution to $n(\lambda)$ using the values of R from Liou et al.[71] and Fernandez et al.[60] The resulting Sellmeier coefficients for $n(\lambda)$ are given in Table 5.

The fit reported by Fernandez et al.[60] suggests earlier refractive error in the NIR region has been overestimated [see Fig. 7(a)]. Taking the dispersion data from Fig. 7(b) in conjunction with the reduced eye model by Thomas et al.,[62] the spot size at a virtual retina can be predicted. The position of the virtual retina, or focal plane, is chosen to be the position

Table 5 Sellmeier coefficients found to produce a fit to the iterative solution for $n(\lambda)$ [see Fig. 7(b)], based on the refractive error values of the human eye from Liou et al.[71] and Fernandez et al.[60] in Fig. 7(a).

B_1	$7.516 * 10^{-1}$
B_2	$-4.484 * 10^{-3}$
B_3	$-1.503 * 10^{1}$
C_1	$1.641 * 10^{-2}$
C_2	$8.596 * 10^{-2}$
C_3	$-1.028 * 10^{3}$

for where refractive error measurements are referenced or where 589-nm radiation comes to a minimum focus. The diameter of the laser beam due to chromatic dispersion as a function of wavelength was computed and is presented in Fig. 8.

From Fig. 8, the expected $1/e^2$ diameter at the retina from a 1300-nm laser-beam is on the order of 180 μm. However, the predicted diameter of the laser spot on the retina due to chromatic aberrations is strongly dependent on the input parameters, including dispersion and the beam profile being launched into the eye model at the virtual cornea. The beam profile used to generate the data in Fig. 8 was the same as the beam parameters used in the Thomas et al.[62] reduced eye model discussed earlier. The distance between the focal positions of the reference wavelength and the 1300-nm wavelengths can be calculated from the equation for refractive error yielding a distance of ~520 μm for a relaxed, 58D eye. Knowing the retina is ~200 μm thick, the focus of a NIR wavelength reaches into the choroid.

4 Discussion

Retinal damage threshold lesions in the 1300-nm wavelength region characteristically involve the full-retinal thickness and exhibit delayed onset inflammation.[7,35] It helps to understand the nature of 1300-nm retinal damage by considering the
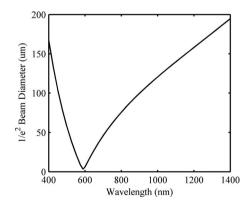

Fig. 8 Predicted spot size at a virtual retinal plane using the information from the reduced eye model in conjunction with the dispersion data from Fig. 7(b).

beam's focus resides in the choroid due to chromatic dispersion and the strong absorptive properties of water in the NIR wavelength region. These basic laser-tissue properties help explain the appearance and extent of damage in the retina from NIR radiation when compared to visible radiation lesions, which are not subject to as extensive chromatic shift and are much more strongly absorbed in the RPE. Linear absorption and chromatic shift alone are unable to explain why retinal damage could not be achieved in the CW 1318-nm radiation studies on the rhesus; instead, our attention is drawn to the nonlinear process of a thermal lens impacting the size of the beam at the retina.

One unexplored laser-tissue interaction between CW NIR radiation and ocular media is the protection of the retina and choroid by a nonlinear thermal lens gradient. The thermal lens causes the focus of the beam to shift posterioraly, increasing the beam size on the retinal plane, and subsequently, decreasing the fluence rate (in watts per centimeter squared) in the neural retina, RPE, and choroid. Lin [23] and Lin et al.[24] has demonstrated how thermal lensing is strongly related to the absorption coefficient suggesting thermal lensing plays a role in tissue optics. It is reasonable to predict significant thermal lensing is present during the CW 1300-nm radiation exposures given the large absorption coefficient of ocular media in the 1300–1340-nm threshold studies.[2]

Laser radiation is attenuated by the four basic compartments of the eye: cornea, aqueous humor, crystalline lens, and vitreous humor. The rabbit has a crystalline lens thickness of 0.79 cm, which is nearly double the lens thickness of the rhesus, 0.40 cm (see Fig. 4). The rhesus has a longer vitreous humor pathlength, 1.23 cm, compared to the rabbit, 0.67 cm. The crystalline lens absorbs the least amount of NIR radiation while vitreous absorbs the most out of the four basic components of the eye (see Fig. 5). The rabbit also has a shorter ocular axial length, 1.79 cm, compared to the rhesus, 1.99 cm. These variations between species allow for more than twice the amount of energy to reach the retina of the rabbit compared to the rhesus for laser radiation in the 1315–1330-nm region (see Table 3). If we neglect variation between the retinas of each species, it would be anticipated that a higher TIE, near a factor of two times the TIE ED_{50} of the rabbit, would be required to cause a retinal lesion in the rhesus. However, at larger TIE, up to the limits of the laser, CW retinal lesions could not be produced in the rhesus (refer to Table 1).

The role of thermal lensing may be a significant laser-tissue interaction influencing the absence of a retinal lesion for wavelengths, where <50% of the TIE reaches the retina, or absorption coefficients begin to reach the order of 1 cm^{-1} (see Figs. 5 and 6). It is in this region where damage to the retina becomes less dependent on RPE absorption and more dependent on the bulk absorbance due to water content. We believe the rhesus' longer vitreous humor pathlength leads to an increased temperature gradient caused by NIR radiation exposure and subsequent increase in thermal lensing compared to the rabbit. The thermal lens would further lower the fluence rate reaching the retina by distributing the NIR laser radiation beam over a larger area. There should be a limit to which the thermal lens would afford protection of the retina and a particular TIE and CW exposure duration, which would
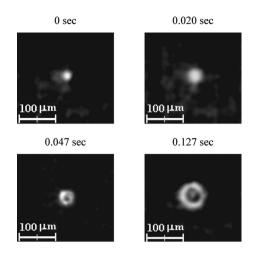

Fig. 9 Changes in a minimum spot formed by a 25.4-mm focal length lens for a 633-nm beam coaligned with a 1313-nm beam passing through a 1-cm thick sample of vitreous (μ_a=1.77 cm^{-1}) at 0, 20, 47, and 127 ms. The laser's diameter in the absorbing media begins to expand nonlinearly with time.[64]

cause damage in the rhesus retina. This limit has yet to be determined.

Typically, the phenomenon of thermal lensing is exploited in a z-scan technique to quantify weak or strong absorbance properties of a liquid or material.[63] Thermal lensing can be easily demonstrated by projecting the transmitted light from a collimated or focused beam through an absorbing medium onto a screen in the farfield. Images of how a focused spot *in vitreous* changes in time are illustrated in Fig. 9. The laser's diameter increases nonlinearly in time to a steady-state condition. The time to reach steady state is dependent on input beam geometry, absorption of radiation in the media, and the power of the beam.[64]

Gordon et al. described the governing equation for changes in the local index of refraction, n, in terms of radial distance vector, $\vec{r}$, from the central axis and temperature rise, ΔT, over time, t, as described in[39]

$$n(\vec{r},t) = n_o + \left(\frac{dn}{dT}\right)\Delta T(\vec{r},t), \qquad (4)$$

where n_o is the background index of refraction at $t=0$. Gordon et al.[39] demonstrated how even a weakly absorbing media with a μ_a of 10^{-3} to 10^{-4} cm^{-1} and a small 0.075 °C increase in temperature resulted in the formation of a thermal lens with a 7.5×10^{-5} change in n from beam center to beam edge. The radial temperature gradient increases as the power and absorption coefficient increase; thus, the strength of the thermal lensing effect is predicted to increase. The decrease in index of refraction as temperature increases in ocular components, combined with the Gaussian radial profile of the laser beam (and thus initially a Gaussian heating profile in the radial direction), creates a negative lens effect.[65]

The time-dependent ratio of d_λ to d_0 as seen in Eq. (2) has been debated based on the value of d_0. It is possible retinal lesions of <80 μm remain unseen by the fundus camera as found in studies by Lund et al.[56] The value of d_0 is subject to variability, including limitations of the ophthalmoscope,

proper training, and experience of the observer, and contrast variations in pigmentation between subjects' retinas lending to lesion appearance.

The value of d_λ needs to be examined as well. The value of d_λ will be dependent on the transient response of the thermal lensing gradient. ED_{50} data in the ultrashort regime represent an impulse response with negligible thermal lensing. Data for NIR radiation CW exposures, however, represent a steady-state response with sufficient time for a thermal lens gradient to form. Although, the time required for the creation of the thermal lens in the eye is not exactly known, we can consider the fact that CW 1318-nm radiation retinal damage was not observed in a rhesus animal model and hypothesize at least microseconds are required for an effective lens to take hold. Initial estimates of the magnitude of the thermal lens from a first-order model with constant coefficients predict a minimum spot of 190 μm will more than double in size in the first 5 ms for TIE at the retinal ED_{50} threshold for CW exposures (Table 1).[66,67] A detailed examination of a thermal lensing model is currently underway.

Retinal damage from the 1150–1350-nm region is primarily associated with direct absorption by water in the retina as opposed to visible wavelengths, where the general belief is that thermal damage is centered on the conduction of heat from the RPE. Thermal lensing increases the retinal spot size beyond the increase predicted by chromatic dispersion models. The action spectra provide reasonable approximations to TIE ED_{50} data when corrections are made for chromatic aberration. However, there is insufficient CW data in the NIR radiation region to know if the present action spectra fit to NIR radiation ED_{50} data accurately. Currently, the Lund et al.[17,21] action spectra do not consider thermal lensing effects.

5 Conclusion

Many laser-tissue mechanisms from an eye exposed to NIR radiation can be explained through the analysis of an action spectrum. These include the strong linear absorbance in ocular tissues leading to decreased transmission to the retina, weaker absorption of NIR radiation in the RPE layer in the retina, and chromatic dispersion in the eye resulting in a larger spot on the retinal surface with damage through the full-retinal thickness. In addition to these mechanisms, thermal lensing affords some protection in the rhesus eye from retinal damage at CW exposures helping to explain the variance in results between rabbit and rhesus retinal damage studies. The protective effect is not unconditional, though the condition for where CW NIR radiation causes retinal damage in a rhesus has yet to be determined. Thermal lensing in the NIR remains an unexplored mechanism in ocular media. It is left to be seen what magnitude the thermal lensing effect has in the eye in protecting the retina and choroid from damage.

References

1. E. A. Boettner and J. R. Wolter, "Transmission of the ocular media," *Invest. Ophthalmol.* **1**(6), 776–783 (1962).
2. E. F. Maher, "Transmission and absorption coefficients for the ocular media of the Rhesus monkey," in SAM -TR-78-32, pp. 1–104, USAF School of Aerospace Medicine (1978).
3. T. J. T. P. van den Berg and H. Spekreijse, "Near infrared light absorption in the human eye media," *Vision Res.* **37**(2), 249–253 (1997).
4. J. T. Walsh, "Pulsed laser angioplasty: A paradigm for tissue ablation," 25 in *Optical-Thermal Response of Laser-Irradiated Tissue*, A. J. Welch and M. J. C. van-Gemert, Eds., pp. 889–893, Plenum Press, New York (1995).
5. D. J. Lund, P. R. Edsall, D. R. Fuller, and S. W. Hoxie, "Bioeffects of near-infrared lasers," *J. Laser Appl.* **10**(3), 140–143 (1998).
6. J. A. Zuclich, D. J. Lund, B. E. Stuck, and P. R. Edsall, "Ocular effects and safety standard implications for high-power lasers in the 1.3–1.4 mm wavelength range," in Tech. Report, pp. 1–16, AFRL/HEDO, San Antonio (2004).
7. J. A. Zuclich, D. J. Lund, and B. E. Stuck, "Wavelength dependence of ocular damage thresholds in the near-IR to far-IR transition region: Proposed revisions to MPEs," *Health Phys.* **92**(1), 15–23 (2007).
8. J. A. Zuclich, D. J. Lund, P. R. Edsall, R. E. Stuck, and G. Hengst, "Highpower lasers in the 1.3- to 1.4-mm wavelength range: ocular effects and safety standard implications," *Proc. SPIE* **4246**, 78–88 (2001).
9. J. A. Zuclich, D. A. Gagliano, F. Cheney, B. E. Stuck, H. Zwick, P. Edsall, and D. J. Lund, "Ocular effects of penetrating IR laser wavelengths," *Proc. SPIE*, **2391**, 112–125 (1995).
10. D. J. Lund, B. E. Stuck, and E. S. Beatrice, *Biological Research in Support of Project MILES*, 96, pp. 1–54, Letterman Army Institute of Research, Presidio of San Francisco, CA (1981).
11. B. E. Stuck, D. J. Lund, and E. S. Beatrice, "Ocular effects of laser radiation from 1.06 to 2.06 mm," Letterman Army Institute of Research, San Francisco, CA (1980)..
12. ANSI, *American National Standard for Safe Use of Lasers, Z136.1*, Laser Institute of America, Orlando (2000).
13. ICNIRP, "Revision of guidelines on limits of exposure to laser radiation of wavelengths between 400 nm and 1.4 microns," *Health Phys.* **79**(4), 431–440 (2000).
14. R. Brancato, R. Praresi, G. Leoni, G. Trabucchi, and U. Vanni, "Histopathology of diode and argon laser lesions in rabbit retina," *Invest. Ophthalmol. Visual Sci.* **30**(7), 1504–1510 (1989).
15. A. Yumita, S. Shirato, and Y. Kitazawa, "Retinal damage threshold of ophthalmic Q-switched ND-YAG laser in monkey eyes," *Jpn. J. Ophthalmol.* **30**(1), 100–115 (1986).
16. C. P. Cain, C. P. Toth, G. D. Noojin, D. J. Stolarski, D. J. Payne, and B. A. Rockwell, "Visible lesion threshold dependency on retinal spot size for ultrashort laser pulses in the near infrared," *Proc. SPIE*, **3254**, 126–129 (1998).
17. D. J. Lund, P. Edsall, and B. E. Stuck, "Spectral dependence of retinal thermal injury," *Proc. SPIE*, **3902**, 22–34 (2000).
18. G. Polhamus, J. Zuclich, C. Cain, R. Thomas, and M. Foltz, "Model predictions of ocular injury from 1315 nm laser light," *Proc. SPIE* **4953**, 91–100 (2003).
19. J. A. Zuclich, P. R. Edsall, D. J. Lund, B. E. Stuck, R. C. Hollins, S. Till, P. A. Smith, L. N. McLin, and P. K. Kennedy, "Variation of laser induced retinal-damage threshold with retinal image size," *J. Laser Appl.* **12**(2), 74–80 (2000).
20. R. A. Glickman, "Phototoxicity to the retina: Mechanisms of damage," *Int. J. Toxicol.* **21**(6), 473–490 (2002).
21. D. J. Lund and P. Edsall, "Action spectrum for retinal thermal injury," *Proc. SPIE*, **3591**, 324–334 (1999).
22. L. A. Priebe, C. P. Cain, and A. J. Welch, "Temperature rise required for production of minimal lesions in the Macaca mulatta retina," *Am. J. Ophthalmol.* **79**(3), 405–412 (1975).
23. W. C. Lin, "Dynamics of tissue optics during laser heating," Doctoral dissertation, University of Texas (1997).
24. W. C. Lin, M. Motamedi, and A. J. Welch, "Nonlinear optical behavior of ocular tissue during laser irradiation," *Appl. Opt.* **34**(34), 7979–7985 (1995).
25. J. A. Zuclich, P. R. Edsall, D. J. Lund, B. E. Stuck, R. C. Hollins, S. Till, P. A. Smith, L. N. McLin, and P. K. Kennedy, "Variation of laser induced retinal-damage threshold with retinal image size," *J. Laser Appl.* **12**(2), 78–80 (2000).

26. M. F. Blankenstein, J. Zuclich, R. G. Allen, H. Davis, S. J. Thomas, and R. F. Harrison, "Retinal hemorrhage thresholds for Q-switched neodymium-Yag laser exposures," *Invest. Ophthalmol. Visual Sci.* **27**(7), 1176–1179 (1986).

27. R. Birngruber, V. P. Gabel, and F. Hillenkamp, "Experimental studies of laser thermal retinal injury," *Health Phys.* **44**(5), 519–531 (1983).

28. G. W. Mikesell, Jr., "Corneal temperatures—A study of normal and laser injured corneas in the Dutch belted rabbit," *Am. J. Optom. Physiol. Opt.* **55**(2), 108–115 (1978).

29. D. Peri, J. Turetz, E. Fishbine, I. Egoz, T. Kadar, and R. Brandeis, "Optical system for exposure of rabbit eyes to laser light and in-situ assessment of retinal damage," *Proc. SPIE*, **6138**, 339–403 (2006).

30. G. Polhamus, and A. J. Welch, "Effect of pre-exposure fundus temperature on threshold lesion temperatures in the laser-irradiated rabbit retina," *Invest. Ophthalmol.* **14**(7), 562–565 (1975).

31. C. P. Cain and G. D. Noojin, "A comparison of various probit methods for analyzing yes/no data on a log scale," USAF Armstrong Laboratory, Brooks City-Base, Texas, AL/OE-TR-1996-0102 (1996).

32. R. Henderson and K. Schulmeister, *Laser Safety*, Institute of Physics, Philadelphia, (2004).

33. D. J. Lund, P. Edsall, and B. E. Stuck, "Wavelength dependence of laser-induced retinal injury," *Proc. SPIE*, **5688**, 383–393 (2005).

34. L. A. Priebe and A. J. Welch, "Asymptotic rate process calculations of thermal injury to the retina following laser irradiation," *J. Biomech. Eng.* **100**(1), 49–54 (1978).

35. J. A. Zuclich, S. T. Schuschereba, H. Zwick, S. A. Boppart, J. G. Fujimoto, F. E. Cheney, and B. E. Stuck, "A comparison of laser-induced retinal damage from infrared wavelengths to that from visible wavelengths," *Lasers Light Ophthalmol.* **8**(1), 15–29 (1997).

36. J. A. Zuclich, M. F. Blankenstein, S. J. Thomas, and R. F. Harrison, "Corneal damage induced by pulsed CO2 laser radiation," *Health Phys.* **47**(6), 829–835 (1984).

37. J. A. Zuclich, H. T. Zwick, S. T. Schuschureba, B. E. Stuck, and F. E. Cheney, "Ophthalmoscopic and pathologic description of ocular damage induced by infrared laser radiation," *J. Laser Appl.* **10**(3), 114–120 (1998).

38. J. A. Zuclich, S. Schuschereba, H. Zwick, F. Cheney and B. E. Stuck, "Comparing laser-induced retinal damage from IR wavelengths to that from visible wavelengths," *Proc. SPIE*, **2674**, 66–79 (1996).

39. J. P. Gordon, R. C. Leite, R. S. Moore, S. P. Porto, and J. R. Whinnery, "Long transient effects of lasers with inserted liquid samples," *J. Appl. Phys.* **36**(3), 3–8 (1965).

40. N. E. Fishkin, J. R. Sparrow, R. Allikmets, and K. Nakanishi, "Isolation and characterization of a retinal pigment epithelial cell fluorophore: An all-trans-retinal dimer conjugate," *Proc. Natl. Acad. Sci. U.S.A.* **102**(20), 7091–7096 (2005).

41. J. B. Nofsinger and J. D. Simon, "Radiative relaxation of sepia eumelanin is affected by aggregation," *Photochem. Photobiol.* **74**(1), 31–37 (2001).

42. J. B. Nofsinger, S. E. Forest, and J. D. Simon, "Explanation for the disparity among absorption and action spectra of eumelanin," *J. Phys. Chem. B* **103**(51), 11428–11432 (1999).

43. G. Eldred and M. Katz, "Fluorophores of the human retinal pigment epithelium: Separation and spectral characterization," *Exp. Eye Res.* **47**(1), 71–86 (1988).

44. A. Vitkin, J. Woosley, B. Wilson, and R. R. Anderson, "Optical and thermal characterization of natural (Sepia officinalis) melanin," *Photochem. Photobiol.* **59**(4), 455–462 (1994).

45. O. Strauss, "The retinal pigment epithelium in visual function," *Physiol. Rev.* **85**(3), 845–881 (2005).

46. V. P. Gabel, R. Birngruber, and F. Hillencamp, "Visible and near infrared light absorption in pigment epithelium and choroid," in *XXIII Concilium Ophthalmologicum (Reprinted from the International Congress Series No. 450)*, K. Shimizu, Ed., pp. 658–662, Excerpta Medica, Amsterdam (1978).

47. P. S. Coogan, W. F. Hughes, and J. Mollson, "Histologic and spectrophotometric comparisons of the human and rhesus monkey retina and pigmented ocular fundus," USAF School of Aerospace Medicine, Rush-Presbyterian St. Lukes Medical Center (1974).

48. W. J. Geeraets, R. C. Williams, G. Chan, W. T. Ham Jr., D. Guerry III, and F. H. Schmidt, "The relative absorption of thermal energy in retina and choroid," *Invest. Ophthalmol.* **1**(3), 340–347 (1962).

49. W. J. Geeraets, R. C. Williams, G. Chan, W. T. Ham Jr., D. Guerry III, and F. H. Schmidt, "The loss of light energy in retina and choroid," *Arch. Ophthalmol. (Chicago)* **64**(1), 158–167 (1960).

50. R. Birngruber, F. Hillenkamp, and V. P. Gabel, "Theoretical investigations of laser thermal retinal injury," *Health Phys.* **48**(6), 781–796 (1985).

51. D. J. Lund, P. Edsall, and B. E. Stuck, "Spectral dependence of retinal thermal injury," *J. Laser Appl.* **20**(2), 73–82 (2008) .

52. A. Hughes, "A schematic eye for the rabbit," *Vision Res.* **12**(1), 123–138 (1972).

53. A. Fernandes, D. V. Bradley, M. Tigges, J. Tigges, and J. G. Herndon, "Ocular measurements throughout the adult life span of rhesus monkeys," *Invest. Ophthalmol. Visual Sci.* **44**(6), 2373–2380 (2003).

54. G. M. Hale and M. R. Querry, "Optical constants of water in the 200-nm to 200-mm wavelength region," *Appl. Opt.* **12**(3), 555–563 (1973).

55. J. A. Zuclich, D. J. Lund, P. E. Edsall, S. Till, B. E. Stuck, R. C. Hollins, and P. K. Kennedy, "New data on the variation of laser-induced retinal damage threshold with retinal image size," *Proc. of Laser Bioeffects Meeting*, Paris, 2002 (unpublished), pp. 3:1–19.

56. D. J. Lund, P. Edsall, B. E. Stuck, and K. Schulmeister, "Variation of laser-induced retinal injury thresholds with retinal irradiated area: 0.1-s duration, 514-nm exposures," *J. Biomed. Opt.* **12**(2), 024023 (2007).

57. J. A. Zuclich, D. J. Lund, P. R. Edsall, R. C. Hollins, P. A. Smith, B. E. Stuck, and L. N. McLin, "Experimental study of the variation of laser-induced retinal damage threshold with retinal image size," *Mol. Cryst. Liq. Cryst. Sci. Technol., Sect. B: Nonlinear Opt.* **21**(1–4), 19–28 (1999).

58. G. Wald and D. R. Griffen, "The change in refractive power of the eye in dim and bright light," *J. Opt. Soc. Am.* **37**(5), 321–326 (1947).

59. R. E. Bedford and G. Wyszecki, "Axial chromatic aberration of the human eye," *J. Opt. Soc. Am.* **47**(6), 564–565 (1957).

60. E. J. Fernández, A. Unterhuber, P. M. Prieto, B. Hermann, W. Drexler, and P. Artal, "Ocular aberrations as a function of wavelength in the near infrared measured with a femtosecond laser," *Opt. Express* **13**(2), 400–409 (2005).

61. "Aberrations of optical images" and "The eye as an optical system," Chapters 7 and 8 in *The Eye: Visual Optics and the Optical Space Sense*, H. Davson, Ed., pp. 87–99, Academic Press, New York (1962).

62. R. J. Thomas, R. L. Vincelette, C. D Clark III, J. Stolarski, L. J. Irvin, and G. D. Buffington, "Propagation effects in the assessment of laser damage thresholds to the eye and skin," *Proc. SPIE*, **6435** 64350–A-1 (2007).

63. M. Franko and C. D. Tran, "Analytical thermal lens instrumentation," *Rev. Sci. Instrum.* **67**(1), 1–18 (1996).

64. R. L. Vincelette, R. J. Thomas, B. A. Rockwell and A. J. Welch, "Thermal lensing in the ocular media," *Proc. SPIE*, **6435**, 64350c (2007).

65. A. Yariv, *Quantum Electronics*, Wiley, Hoboken, NJ (1989).

66. R. L. Vincelette, R. J. Thomas, B. A. Rockwell, and A. J. Welch, "A comparison of a first-order thermal lensing model to a closed aperture Z-scan for the propagation of light in ocular media," *Proc. SPIE*, **6084**, 0G1–0G9 (2006).

67. R. J. Thomas, R. L. Vincelette, G. D. Buffington, A. D. Strunk, M. A. Edwards, B. A. Rockwell, and A. J. Welch, "A first order model of thermal lensing of laser propagation in the eye and implications for laser safety," *International Laser Safety Conference*, D. Sliney, Ed., pp. 147–154 Laser Institute of America (2005).

68. D. J. Lund, P. Edsall, and B. E. Stuck, "Ocular hazards of Q-switched near-infrared lasers," *Proc. SPIE*, **4953**, 85–90 (2003).

69. G. Li, H. Zwick, B. Stuck, and D. J. Lund, "On the use of schematic eye models to estimate retinal image quality," *J. Biomed. Opt.* **5**(3), 307–314 (2000).

70. G. Westheimer, *The Eye: Including Central Nervous System Control of Eye Movements*, C.V. Mosby Company, St. Louis, MO (1980).

71. H. L. Liou and N. A. Brennan, "Anatomically accurate, finite model eye for optical modeling," *J. Opt. Soc. Am. A* **14**(8), 1684–1695 (1997).

72. D. A. Atchison and G. Smith, "Chromatic dispersions of the ocular media of human eyes," *J. Opt. Soc. Am. A* **22**(1), 29–37 (2005).